ISSN 1330-3651 (Print), ISSN 1848-6339 (Online)
Received: 28 March 2025; Accepted: 26 December 2025

https://doi.org/10.17559/TV-20250328002529
Original scientific paper

Analysis of Concrete Blocks with Rubber and Recycled Glass and Their Use in Low-Rise Structures

D. DOMINGUEZ-SANTOS, Francisca E. SEPÚLVEDA LAGOS

Abstract: Concrete blocks are one of the most widely used construction elements in the world of construction, due to their good mechanical behaviour, easy placement and versatility in structures, enclosures and partitions. Despite their good construction characteristics, their defects involve their flexural-tensile strength behaviour and their thermal and waterproof behaviour. This research aims to improve these behaviours, using materials that improve these properties but without making the product more expensive and respecting the environment, as the glass and the rubber is recycled. The different laboratory tests carried out (mechanical, thermal and waterproof) show how small quantities (0.625%, 1.250% and 2.500% by mass instead of sand and gravel) of these recyclable materials improve the most deficient properties of the traditional block. It is demonstrated that the use of these new blocks improves the structural and thermal properties of the traditional block, computationally in a three-dimensional three-storey model.

Keywords: concrete; concrete blocks; frame structures; recycled aggregate; recycled glass; recycled rubber

1 INTRODUCTION

The high levels of structural, waterproof and thermal requirements in construction are the result of technological advances and technical improvements introduced by the requirements of building regulations, seeking more effective, more efficient and more economical solutions for the well-being of people. In addition to this, in recent years, society has demanded the need to use more sustainable materials. Construction is responsible for a significant part of the generation of polluting waste, which significantly affects the well-being of society and the development of countries [1]. To mitigate this environmental impact, priority is given to choosing less polluting materials [2], incorporating other criteria in construction, such as sustainability and economy [3].

All of this has led to the investigation and study of materials and construction elements, to optimise their characteristics and try to improve the most deficient properties, complying with the high standards required by the standards in different countries [4], while improving the quality of the environment by re-using highly polluting disposable materials.

Of all the construction materials studied, concrete is one of the most widely used materials in the world due to its great versatility in construction, not only in finishes (enclosures, partitions, floors etc.) but also in structures. It is a material with good properties and construction characteristics but it does have some deficiencies, such as its thermal behaviour, mechanical behaviour in terms of flexural-tensile strength or its high polluting rate on the environment during its production [60-62].

One of the processes meeting sustainable conditions, related to environmental protection and the overexploitation of raw materials, is recycling (Global Recycling Foundation [63]). That is why minimising high energy consumption in the production and manufacturing of highly polluting materials such as concrete, contributing to improving energy efficiency, is done through the introduction of new materials to the chemical composition of the original materials [5, 6].

There are studies of additives being incorporated into traditional concrete, seeking to improve some of these deficient characteristics such as, for example, resistance or durability, by reducing the amount of cement and CO_2 emissions, thus favouring sustainable construction [7]. In addition to this, there are other studies that seek to improve other characteristics, such as the thermal properties of concrete [8], acoustic properties [9], durability, mechanical and waterproof properties [10].

The novelty in this research lies in the development and performance of laboratory testing of prefabricated concrete blocks, incorporating rubber fibres and recycled glass in their composition, and analysing their properties, instead of analysing the concrete as a material, using these additives [49, 50, 57-59]. Finally, the results of the laboratory tests are used in the structural and energy modelling of a building, comparing it with traditional blocks. The main novelty of this research lies in the inclusion of both materials acting together, a topic not extensively studied in the scientific literature [78-85]. Furthermore, the decision to use concrete block specimens instead of cubic or rectangular concrete specimens introduces a novel approach to the analysis of the structural, waterproofing (absorption), and thermal behavior of a widely used construction element: walls and partitions. Moreover, modeling the element within a frame structure, using the mechanical values obtained in the laboratory, and analyzing its structural behavior makes this a more innovative, unique, and practical study).

2 MATERIALS AND METHODS

2.1 Sample Manufacturing

For the production and testing of concrete blocks, the following regulations were considered:

1. NCh181 (2006) [11]. Concrete blocks for structural use - General requirements. This standard establishes the requirements that concrete blocks must meet for structural use, classifying them according to the density of the mixture.
2. NCh182 (2007) [29]. Concrete blocks for structural use - Trials. This document establishes the test methods for structural concrete blocks.

3. NCh853 (2007) [31]. Thermal conditioning - Thermal envelope of buildings - Calculation of thermal resistance and transmittance.
4. NCh1038 (2009) [30]. Flexural-tensile strength test. This standard establishes the flexural-tensile strength test procedures.
5. NCh1498 (2012) [74]. Concrete and mortar - Mixing water - Classification and requirements. This standard establishes the classification and requirements of the waters that must be used in the mixing of concrete and mortar.
6. NCh163 (2013) [75]. Aggregates for mortar and concrete - Requirements. This standard specifies the properties of aggregates to produce mortar and concrete.
7. NCh170 (2016) [12]. Concrete - General requirements. This standard designates the minimum general requirements that must be considered to classify concretes according to their compressive or tensile strength. In addition, it establishes how the stages for the manufacture of concrete must be executed, depending on its density.
8. NCh148 (2016) [76]. Cement - terminology, classification and general specifications. This standard specifies and classifies the cements used in concretes.

To determine the dosage of the concrete used in the blocks, the Faury-Joisel method [64] was used based on granulometric principles. This involves obtaining a granulometric curve referring to the process, known as (*L*). In this process, cement is combined with the available aggregates and the curve is obtained by the nominal maximum size of the coarse aggregate (*Dn*) and the desired concrete strength, known as design strength (*fd*), at 28 days.

The ideal curve *L* (Fig. 4) is represented by a graph made up of two coordinate axes (*X*, *Y*). The abscissa axis (*X*) represents the fifth root of the sieve opening occupied by the aggregate granulometry, expressed in mm. On the other hand, the ordinate axis (*Y*) represents the percentage of absolute volume of solid materials on a linear scale.

In this study, hollow structural blocks were made with the dimensions stipulated in NCh181. For the manufacture of the external formwork of the hollow concrete blocks, an 18 mm thick phenolic sheet was used. Inside, hollows were made of expanded polystyrene, as shown in Fig. 1. The resulting hollow concrete block had the dimensions 39 × 19 × 19 cm^3, complying with the provisions of NCh181.

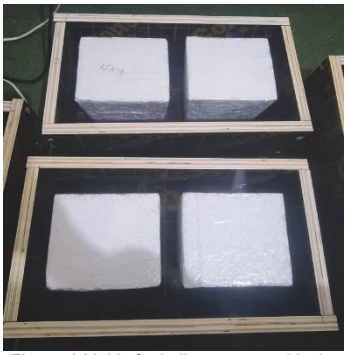

Figure 1 Molds for hollow concrete blocks

Having described the production of traditional concrete blocks in compliance with the regulations, the dosage and selection of aggregates incorporated into the concrete mixtures in the blocks was justified. The choice of the two materials used in this research (for the new concrete dosage) resulted from the improvement of the most deficient properties of traditional concrete. With recycled glass, the aim was to improve the thermal and resistant properties while, with recycled rubber, the aim was to improve the thermal insulation, the flexural-tensile strength behaviour, the durability and the permeability. The choice of these materials was influenced by the existing amount of waste of these materials, with the aim of reusing them and helping the environment.

All the samples were taken at the same time, so that the climatic variations which could affect the resistance of the blocks did not occur. Likewise, the origin of all the materials used in the composition of the blocks was the same in all cases. The purpose of using materials from the same source, as well as similar environments, temperatures, and testing times, is to avoid discrepancies in the results obtained, since the properties of materials differ greatly depending on their exposure conditions and chemical composition. Variations in any of these factors, especially the origin of the materials, could have caused significant discrepancies in the results.

Based on the background and the existing scientific literature on the incorporation of rubber and recycled glass in the concrete mixture, it is concluded that the incorporation of additives in large proportions (by volume) significantly affects its resistance, due to the greater amount of recycled material used in the manufacture of the blocks. Because of this, the dosages used for these aggregates were specified in relation to their weight [65], justifying what was established in NCh170 [12].

The use of recycled glass in the mixture (from glass bottles) replaced the sand. The size of the glass particles was between 2.50 and 4.75 mm in diameter, achieving a homogeneous mixture. Fig. 2 shows the crushed glass used in the mixtures. For this addition, previous studies and research were followed [14-20].

Figure 2 Recycled glass granules

On the other hand, recycled rubber from tyres replaced the coarse aggregate so that they adhered correctly, obtaining a homogeneous mixture. The size of the rubber particle fibres was between 0.60 and 2.50 mm, with a fibre length between 30 and 33 mm. Fig. 3 shows the crushed rubber (fibres) used in the mixtures. For this replacement material, previous studies and research include [21-28].

For this research, three dosages of these two additives (rubber and glass) were tested, limiting the quantities according to those described in other research, with the aim of finding more optimal solutions in terms of sustainability, while improving the most deficient properties of concrete.

In all mixtures, the same proportion of glass and rubber were used: 0% (traditional concrete Block A), 0.625% (Block B), 1.25% (Block C) and 2.50% (Block D).

Figure 3 Recycled rubber fibres

A total of 24 samples were taken, 6 of each type (A-D). Of these, 3 will be tested in compression and 3 in flexural tensile strength. Prior to these destructive tests, non-destructive tests will be performed on the samples: thermal permeability tests and workability tests (consistency of fresh concrete, by the slump test, UNE-EN 12350-2).

Finally, the tests carried out proved that the compressive and flexural-tensile strength of the concrete, as well as the moisture absorption of the blocks, met the minimums established by NCh181. In the same way, it was proven that the thermal characteristics met the criteria established by the Ministry of Housing and Urban Development (MINVU) and the regulations of the General Urban Planning and Construction Ordinance (OGUC) of Chile.

3 SAMPLES ASSESSMENT

3.1 Results and Properties of the Concretes Used in the Blocks

To determine the production of different concretes, the following results are established:

The curve (*L*) used in the granulometry of the manufactured concrete is the one shown in Fig. 4.

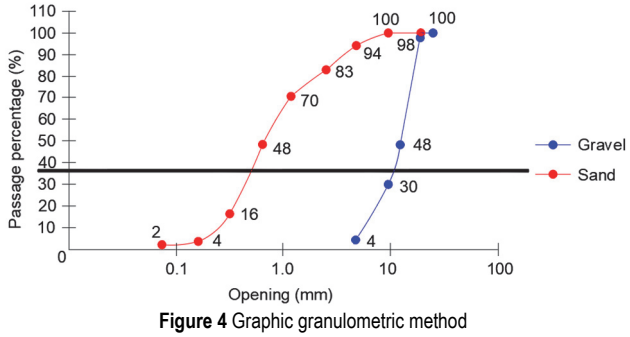

Figure 4 Graphic granulometric method

Once the granulometry of the different materials that make up the concretes had been determined, the quantities (by weight and volume) corresponding to 1 m^3 of traditional concrete were as shown in Tab. 1 and the quantities (by weight) of each material used for each block were as shown in Tab. 2.

Once the quantities of the materials used in each of the blocks were determined, the densities and average masses of each of them were as presented in Tab. 3. Considering the classification of the weights of the concretes in NCh181, all the blocks are classified as 'Normal', i.e. concretes with densities greater than 2000 kg/m^3. As shown in Tab. 3, the inclusion of rubber and glass in the mixtures decreases the density and, therefore, the weight of the concretes. In addition, the percentages of weight reduction are shown in parentheses, compared to the traditional Block A, with the blocks being reduced by up to 8%.

Table 1 Quantities of materials used in traditional block concrete (A)

Material	Quantity in Weight / kg	Quantity in Volume / m^3
Gravel (G)	1075.06	0.405
Sand (F)	640.07	0.247
Cement (C)	441.82	0.143
Water (A)	203.40	0.203

Table 2 Dosage (mass) of the glass and rubber in concretes in each of the blocks (A-D)

Materials	Block A (0%)	Block B (0.625%)	Block C (1.25%)	Block D (2.50%)
Gravel (G) / kg	8.12	8.10	8.08	8.04
Sand (F) / kg	4.84	4.80	4.78	4.71
Cement (C) / kg	3.34	3.34	3.34	3.34
Water (A) / kg	1.54	1.54	1.54	1.54
Rubber fibers / g	0.00	23	44	89
Glass granules / g	0.00	33	65	125

Table 3 Average physical properties of the blocks

Block A		Block B		Block C		Block D	
Mass / kg	Density / kg/m^3	Mass / kg	Density / kg/m^3	Mass / kg	Density / kg/m^3	Mass / kg	Density / kg/m^3
21.46	2360.35	20.99	2308.64 (−2%)	20.57	2262.45 (−5%)	19.91	2189.86 (−8%)

To determine the docility of the fresh concretes in this investigation, the 'Abrams Cone' slump test was used. Tab. 4 shows the slumps and classification of the concrete used for each of the blocks, according to NCh170. Traditional concrete (A) has a soft docility, while concretes with rubber and glass additives in the mixtures (B-D) make the samples more compact, classifying them as having plastic docility. Fig. 5 shows some of the tested block specimens.

Table 4 Docility of each mixture

Concrete type	Cone settlement / cm	Determination of docility NCh170
Concrete A (0%)	6.3	6-9 (Soft)
Concrete B (0.625%)	5.2	3-5 (Plastic)
Concrete C (1.25%)	4.1	3-5 (Plastic)
Concrete D (2.5%)	3.3	3-5 (Plastic)

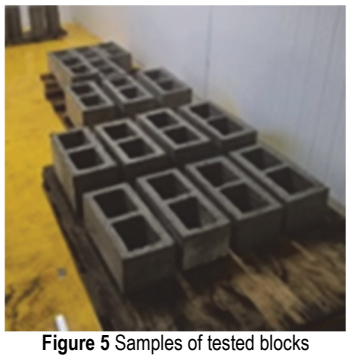

Figure 5 Samples of tested blocks

Fig. 6 shows some images of the docility tests performed with the Abrams cone.

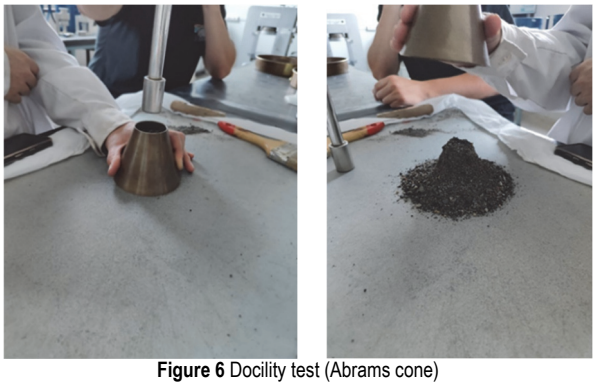

Figure 6 Docility test (Abrams cone)

3.2 Compression Strength Tests

The procedure for this test was carried out in accordance with the NCh 182 standard [29]. After carrying out a drying process on the facing of the contact surfaces of the block, two 10 mm thick metal plates were placed. These smooth and flat metal plates allowed a uniform distribution of the load of the hydraulic press (Fig. 7). Once the block was placed in the machine and the height and base dimensions were noted, the compression strength testing began, applying an incremental and uniform load at a constant speed of 0.25 MPa/s ± 0.05 MPa/s, until failure of the block. The tests were carried out after 28 days of drying, when the concrete reached its maximum strength. The results obtained, the average of 3 samples tested for each of the types of Block tested will be calculated, which is shown in Tab. 7.

Figure 7 Hydraulic press used in the compression strength tests

3.3 Flexural-Tensile Strength Tests

The procedure for this test was carried out as established in the NCh1038 standard [30]. As with the compression strength test, the mass, height, and width were recorded, marking the two contact points that the machine used to apply the load, as shown in Fig. 8. Once the block was installed in the machine, the incremental load started at a constant speed, between 0.86 and 1.21 MPa/min, until the block failed. The tests were carried out after 28 days of drying, when the concrete reached its maximum strength. The results obtained, the average of 3 samples tested for each of the types of Block tested will be calculated, which is shown in Tab. 8.

Figure 8. Hydraulic press used in the flexural-tensile strength tests

3.4 Thermal Tests

To measure the thermal transmittance of the block, a hermetic container was specifically designed for the concrete block (Fig. 9a). Placing the block in the container allowed one of the side faces of the block to be exposed to the outside environment, thus measuring the temperature variations between the outside and the inside of the insulated container. The measurement of each block was measured through three sensors in contact with the block, which were connected to a TESTO 435-2 measuring device (Fig. 9b), responsible for recording and transmitting the measurement values to a computer. The outside temperature was determined with another wireless device that transmitted the measurement data via Bluetooth to the TESTO 435-2 device.

(a) Hermetic container for thermal testing

(b) TESTO 435-2 device

Figure 9 Thermal tests

To obtain reliable results, a temperature difference of about 15 ºC between the outside and inside was ensured. With this value (transmittance), the conductivity and thermal resistance of each block (NCh853 [31]) was calculated, considering its thickness.

All measurements were taken using a sealed container with 5-8 cm thick expanded polystyrene walls (Fig. 9a), leaving the block face exposed. Three measuring sensors were attached to this block and connected to the TESTO 435-2 device (Fig. 9b) and a computer. A temperature difference of 15 °C between the inside and outside of the container was ensured. This device has proven successful in professional applications for measuring the thermal transmittance of building envelopes. It complies with UNE-ISO 9869-1 "Thermal insulation. Building elements.

In-situ measurement of thermal resistance and transmission: heat flow meter method". Furthermore, the device manuals mention the use of ASTM standards (C1046 and C1155) for on-site measured U-value, although these standards are not as common as ISO 9869. This device, with its U-value probe, measures three temperatures: interior, exterior, and the surface of the building envelope, recording the heat flow to automatically calculate the U-value. Additionally, Testo Industrial Services is accredited according to ISO/IEC 17025, through which the devices are calibrated.

3.5 Permeability Test

To measure the moisture absorption of each sample, water absorption and capillarity testing of the blocks were carried out according to the process detailed in the NCh182 standard [29].

Water absorption. To perform this test, three samples of complete blocks were made and marked, recording their mass. For the process, the test pieces were immersed in water at a temperature between 15 and 27 ºC, for a period of 24 hours. These test pieces (Fig. 10) were suspended by a metal wire inside a metal basket, recording the submerged mass (W_i). After 24 hours, they were removed from the water and left to drain for a minute, placing them on a sieve with an opening of 9.5 mm. Subsequently, the visible water was removed from the surface with a damp cloth, recording the saturated mass (W_s). After performing the saturation process, the test pieces were dried in an oven at a temperature between 100 and 115 ºC for 24 hours. After this time, the constant mass (W_d) of each test piece was recorded.

Figure 10 Water absorption test with the block submerged

Capillary absorption. For the measurements of the execution of this test, the three marked blocks were used, recording their mass, being dried in an oven at a temperature of 70 ± 5 ºC, until reaching a constant mass. Subsequently, the blocks were left to rest, to measure the mass of each one, recording its W_o value, in grams (g). Then, the blocks were immersed in a sheet of water no higher than 5 mm in height. Finally, the weights of each test piece (W_i) were recorded at different times, controlling and recording the amount of water that each block was absorbing

4 BUILDING MODEL

In this study, a three storey building was considered, designed with frame structures (Fig. 11a). The span length between columns was 5 m, with four spans in direction *X* and three spans in direction *Y*. The floor plan dimensions were, therefore, 20 × 15 m^2. The most resistant direction was the *X* direction (where the beams were located); in the *Y* direction, the joints were considered rigid, with resistant frames assumed, i.e. those existing in the perimeter of the building (where the enclosures were located). The floor-to-floor height was 3 m, leading to a total height of 9 m for the three-storey building. The floor plan of each model comprised 12 cm thick unidirectional slabs, which acted as a rigid diaphragm. The covering used in each structural section was 2.5 cm. The arrangement of the concrete block walls were as shown in Fig. 11b.

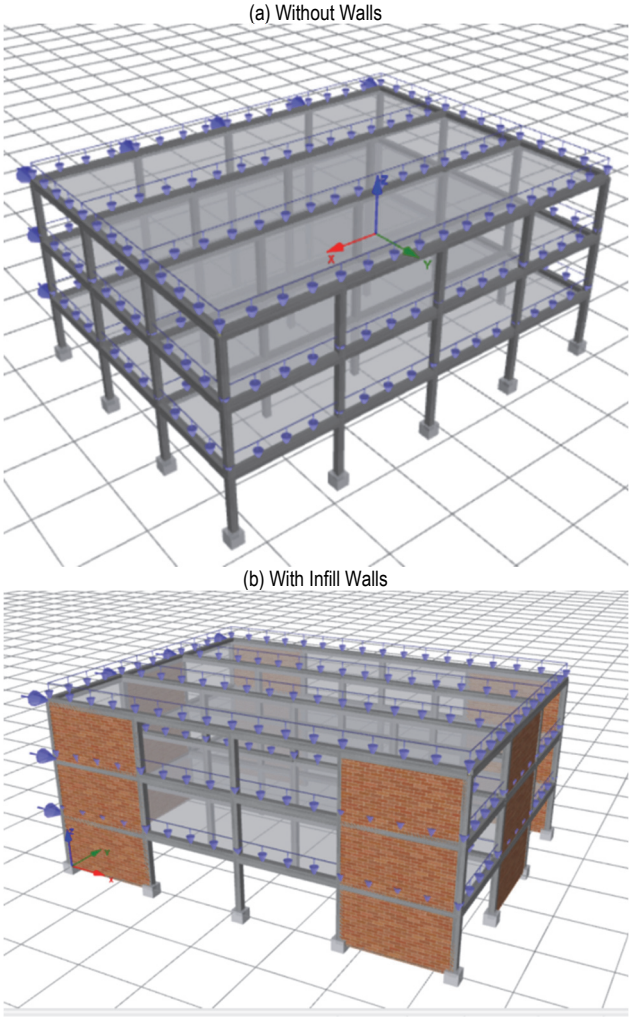

Figure 11 Structural Model

The size of the structural sections used in the beams and columns are shown in Tab. 5. Likewise, the total structural weight of each model, including beams, columns, slabs and infill walls, are shown in Tab. 5. The value in parentheses indicates the weight percentage, with respect to the bare model.

Table 5 Structural sizes and weights for the three-storey building

Case	Beams / cm^2	Columns / cm^2	Weight structure / kN
Bare frame	30 × 40	30 × 30	3767.41
Block A			5108.40 (+36%)
Block B			5079.14 (+35%)
Block C			5046.82(+34%)
Block D			5010.90 (+33%)

The amount of reinforcement used in the sections was between 1.5 and 2.0% of the concrete section. In addition, these reinforcement proportions were designed based on the professional experience of the research team and on regulatory requirements. Thus, for the 30 × 30 cm^2 columns, twelve 16 mm diameter bars were used. As for the 30× 40 cm^2 beams, twelve 16 mm diameter bars were used. Finally, for both columns and beams, stirrups made from 10 mm diameter bars were placed every 15 cm along each element. The steel used for the bars was B500S steel.

5 STRUCTURAL ASSESSMENT

The structural elements were modelled as finite bar elements. Each structural element (columns and beams) was individually characterised, following the prescriptions proposed by Mander for concrete [32] and the Ferrara bilinear model [33] for steel reinforcement.

In particular, the beams were represented by non-linear finite bar elements [34, 35], where the non-linearities are concentrated in the plastic hinge located at the ends of the bars (corresponding to 15% of the total element length) [36]. The model mentioned by Scott et al. [37] was used, where the joints/connections between the concrete columns and beams were rigid and the hysteretic behaviour representing the stress distribution was calculated with fibre models, based on the material properties and the cross section of the structural elements (discretised with 300 fibres). In the model, the loads were applied to the beams. The tolerances used for the displacements and rotations were of the order of 10^{-5} in all cases, with a maximum number of 300 iterations [38].

The simulation of the mechanical behaviour of each material in the frame elements requires the introduction of several data corresponding to the material properties. For this reason, the experimental values of plastification and fracturing obtained from the capacity curves of each of the materials were considered as sufficient. On the other hand, for the unitary deformations corresponding to the fracture processes of the concrete and steel, the standard values of Seismostruct [39-41] were used: concrete cracking (0.0001), concrete spalling (−0.002), concrete fracture (−0.002), yielding (0.0025) and steel fracture (0.06). In addition, the criteria regarding curvature and turns were verified through the rotational capacity of Mergos and Kappos [42] and the cutting capacity established in Eurocode EC-8 [43].

The presence of infill walls considerably modifies the structural behaviour of bare frame structures [66, 67], as shown in the results of this research. For the modelling of the infill wall, the nonlinear inelastic behaviour, the mechanical properties and the interaction with the structure were considered. Among the existing techniques that allow the analysis with infill walls, the procedures of [68-71] were followed, using Seismosoft® software. The double-strut approach adopted by the model was applied for the prediction of the seismic response in reinforced concrete frame structures of various heights. Crisafulli proposed a macromodel that measures the global response of the structures, implementing a four-node 'panel' element connected to the frame at the beam-column connections, as shown in Fig. 12.

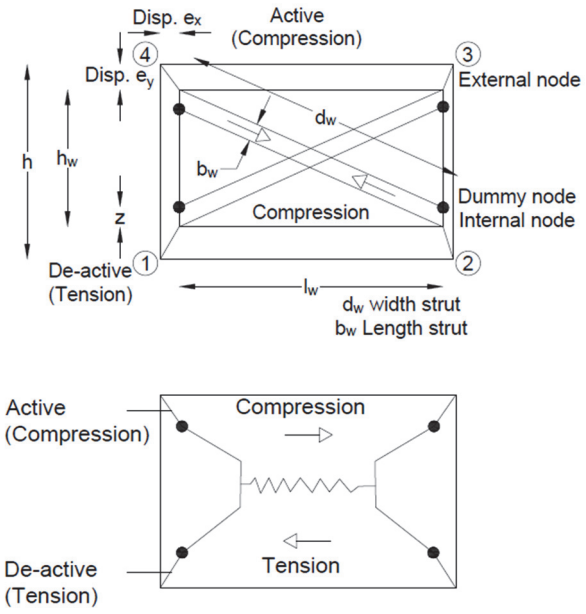

Figure 12 Infill wall Model (Dominguez-Santos and Bravo 2022; SeismoSoft 2020)

Internally, the panel element separately represents the compressive strength and shear behaviour of the block walls [72]. To simulate this behaviour, two parallel struts and a shear spring in each direction were used. This spring allows consideration of the stiffness and lateral resistance of the panel, when a shear failure occurs along the mortar joints or a tensile failure occurs on the expected diagonal. More numerical details of this model can be found in [69, 73]. For the calibration of the model, in terms of infill walls, some geometric and mechanical parameters are required to define the behaviour of the strut used for the blocks. A complete definition of each parameter can be found in [69, 73]. The parameters obtained directly or indirectly in the laboratory tests are shown in Tab. 6. The choice of this calculation method was due to the speed of the computational process, the simplicity of the modelling and because it was chosen in many previous investigations, obtaining good results.

Table 6 Numerical values of the geometry and mechanical behaviour obtained in the laboratory

Units	Block A (traditional block)	Block B	Block C	Block D
t / mm	190	190	190	190
A_1 / mm^2	276970	276970	276970	276970
d_w / mm	5831	5831	5831	5831

Table 6 Numerical values of the geometry and mechanical behaviour obtained in the laboratory - continuation

Units	Block A (traditional block)	Block B	Block C	Block D
b_w / mm	1458	1458	1458	1458
E_b / N/mm^2	7620	8598	8624	7404
b / mm	390	390	390	390
j / mm	12	12	12	12
E_m / N/mm^2	7718	8719	8731	7488
h_w / mm	3000	3000	3000	3000
E_j / N/mm^2	40696	40696	40696	40696
h / mm	2800	2800	2800	2800
f_t / MPa	3.82	4.10	4.32	4.07
$f_{m\theta}$ / MPa	14.10	14.40	13.98	13.75
τ_{max} / MPa	3.10	3.18	3.07	3.00
γ_p / KN/m^3	26.14	25.57	24.94	24.24
h_z / mm	1.48e-05	1.39e-05	1.39e-05	1.50×10^{-5}
θ / °	30.96	30.96	30.96	30.96
I_c / mm^4	675e6	675e6	675e6	675e6

For these analyses, a triangular load was used, distributed along the height of the frames, concentrating the relevant loads at each floor level. These loads were increased by a coefficient λ, resulting in displacements for each case. The displacements obtained for each load increment form the so-called capacity curves that relate the basal shear force with the displacement at the top of the structures [44]. This load was increased until the structure became totally unstable, at which point the calculations were concluded. To perform these calculations, the SEISMOSTRUCT program was used. As mentioned, the nonlinearities of the models are concentrated in the plastic hinges, which facilitate a simpler and faster analysis with good precision [45-48].

5 RESULTS

5.1 Concrete Characteristics

5.1.1 Compression Strength Results

The average results of the compression strength tests of the blocks, considering the Chilean NCh181 Standards, are shown in Tab. 7. This standard establishes a minimum resistance of the three blocks tested for compression strength, for structural use of at least 13 N/mm^2. This indicates that traditional concrete blocks and blocks with recycled rubber and glass aggregates are suitable for structural use. The resistances shown in Tab. 7 do not increase with the amount of rubber and glass in the aggregates but their compressive strength decreases with percentages higher than 1.25%. The values in parentheses in Tab. 7 indicate the percentage with respect to the traditional block (A).

Table 7 Average compression strength results of the blocks

Block type	Recycled Aggregate Value / %	Average Total Strength / N/mm^2	Standard Deviation / N/mm^2
Block A	0	20.03	±0.25
Block B	0.625	22.11 (+10%)	±0.98
Block C	1.25	19.22 (−4%)	±1.19
Block D	2.5	17.77 (−11%)	±0.84

The decrease in compressive strength of blocks C and D is due to the optimization of the quantities of rubber and glass added. Just as glass has greater compressive strength than concrete, rubber has lower strength. Excessive amounts of rubber, combined with the adhesion of both materials to the mix, cause certain quantities to contribute to a decrease in strength. Studies in the scientific literature support this explanation [86-88].

5.1.2 Flexural-Tensile Strength Results

The average results of the flexural-tensile strength tests are shown in Tab. 8 and they show that the incorporation of rubber and glass aggregates increases their strength. The values in parentheses in Tab. 8 indicate the percentage with respect to the traditional block (A).

Table 8 Average flexural-tensile strength results of the blocks

Block type	Recycled Aggregate Value / %	Average Effective Strength / N/mm^2	Standard Deviation / N/mm^2
Block A	0	3.82	±0.10
Block B	0.625	4.10 (+7%)	±0.39
Block C	1.25	4.32 (+13%)	±0.48
Block D	2.5	4.07 (+7%)	±0.61

The decrease in flexural strength of block D is due to the optimization of the amounts of rubber and glass added. The brittle and ductile characteristics of the additives influence the behavior of the blocks. While glass is a highly brittle material, rubber is ductile; therefore, excessive amounts of both materials would negatively affect the behavior of the concrete blocks. Studies in the scientific literature support this explanation [86-88].

5.1.3 Permeability Resistance

This measurement was made according to the procedure indicated in the NCh181 regulations. Fig. 13 shows the results of the water absorption of the concretes used in the blocks, compared to traditional concrete (Block A). The samples with aggregates showed greater impermeability, indicating that the inclusion of a greater quantity of rubber and glass in the mixtures decreases the permeability of the blocks.

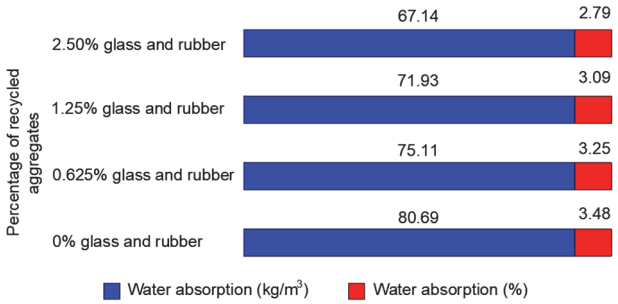

Figure 13 Water absorption test for types of concrete used in hollow blocks

The values obtained in this investigation are the result of a good concrete quality in relation to its hardness, as shown by some existing studies and investigations, where concretes with absorptions of less than 5% are defined as such (Grzegorz Ludwik Golewski in his study [77]).

5.1.4 Thermal Resistance

The results obtained during the thermal testing of the blocks are shown in Tab. 9. This test measures the thermal

transmittance of the blocks (U). With this value, the total thermal resistance (R_T) and its thermal conductivity (λ) are determined, calculated based on the thickness (e), using Eq. (1) and Eq. (2).

- Thermal transmittance:

$$U = \frac{1}{R_T}\left(W / m^2 \cdot K\right) \quad (1)$$

- Thermal conductivity:

$$\lambda = e \cdot U \left(W / m \cdot K\right) \quad (2)$$

Table 9 Thermal test comparison

Block type	Thermal transmittance / W/m²K	Thermal conductivity / W/m × K	Total Resistance / m² × K/W
Block A	2.22	0.42	0.45
Block B	1.81 (−19%)	0.34 (−19%)	0.55 (+22%)
Block C	1.56 (−29%)	0.30 (−29%)	0.64 (+42%)

The results in Tab. 9 show greater thermal insulation of the blocks with recycled rubber and glass aggregates. The values in parentheses show the percentage in relation to the traditional block (A).

The rubber and glass additives introduced into the concrete samples have a significant effect on the thermal properties of traditional concrete due to the expansive effect of both additives in the samples. This, combined with the fact that the thermal characteristics of both elements are significantly superior to traditional concrete, leads to improved thermal conductivity in these new blocks.

5.2 Structural Analysis

Conventional push-over analysis is used to estimate the maximum horizontal resistance capacity of structures that involve a dynamic response.

The incremental load P applied to each floor (rectangular or triangular) is proportional to the nominal load pattern ($P°$) used and defined by the designer on each floor (in this research the load pattern used was triangular) $P = \lambda(P°)$. λ is a factor that proportionally increases the load on each floor until the structure becomes unstable, which is when the program ends the analysis.

The capacity curves obtained from the push-over analysis of the structural model are defined in Fig. 14 and Fig.15, for each direction (X, Y).

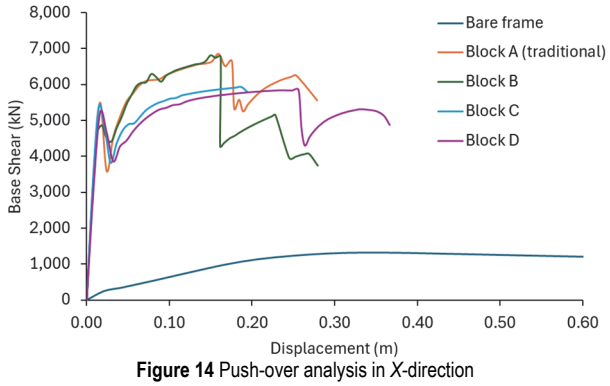

Figure 14 Push-over analysis in *X*-direction

The results show that small amounts of recycled glass and rubber in the production of concrete blocks improve the structural properties of traditional blocks, which is in agreement with other research [49, 50, 57-59].

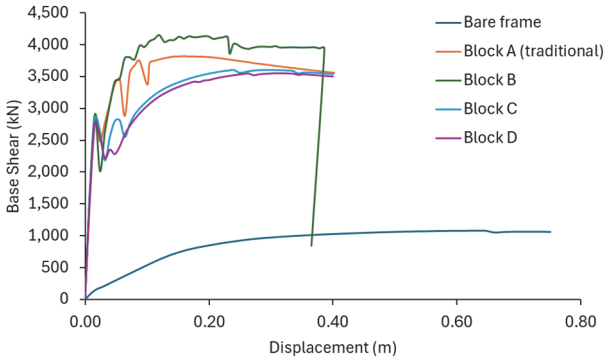

Figure 15 Push-over analysis in *Y*-direction

The most significant values are: F_y (yielding force), F_u (ultimate force), D_y (yielding displacement), D_u (ultimate displacement), μ (ductility) and K_y (yielding stiffness) of the capacity curves of Fig. 14 and Fig. 15. These are shown in Tab. 10.

Table 10 Significant values of the capacity curves

	Bare Frame	Block A	Block B	Block C	Block D
	X/*Y* direction				
F_y / kN	1199/ 931	5756/ 3376	5705/ 3420	4711/ 2753	4703/ 2826
F_u / kN	1329/ 1078	6857/ 3819	6812/ 4149	5931/ 3608	5850/ 3548
D_y / m	0.084/ 0.173	0.054/ 0.044	0.051/ 0.049	0.048/ 0.068	0.051/ 0.076
D_u / m	0.353/ 0.646	0.160/ 0.144	0.150/ 0.108	0.187/ 0.240	0.256/ 0.312
Ductility / μ	4.20/ 3.73	2.94/ 3.26	2.95/ 2.19	3.88/ 3.55	5.02/ 4.09
K_y / kN/m	31254/ 13670	404031/ 212842	436605/ 220681	401647/ 212043	381661/ 201307

As shown in Fig. 14 and Fig. 15 and in the corresponding results for these figures in Tab. 10, the greatest resistances correspond to the X direction (beam direction), the direction in which there is a greater number of infill walls. The initial strength and structural behavior of frame structures with infill walls, as demonstrated in research [89-93], is not due to the main frame elements (columns and beams), but rather to the infill walls. This explains why the strength is not as significant in the X and Y directions, which would have been the case if there had only been beams, since the strength in the weak direction would have been provided by the perimeter beams in the Y direction. In the cases studied, with the presence of infill walls around the perimeter of the structures (exterior walls), the strength will depend on these elements. It is logical that the strength in the weak direction (Y) is 40% lower than in the X direction, due to the number of walls in both directions (8 walls in the X direction and 6 walls in the Y direction).

Furthermore, in this research, through the capacity curves, performance points have been obtained that consider the following aspects in a building: physical damage to structural and non-structural elements, the risks to occupants and the functionality of the service's basic

elements. The California Society of Structural Engineers (SEOAC) (1995) [51], established four levels of performance as a reference:

- Fully operational (no damage): negligible or no structural or non-structural damage.
- Operational (IO): cracks in structural elements. Slight damage.
- Life Safety (LS): moderate damage to some elements. Loss of strength and rigidity of the lateral loaded resistant system. The system remains functional.
- Pre-collapse (CP): severe damage to structural elements. It may be necessary to demolish the building.

To obtain these points, the capacity spectrum method is a widely used procedure for determining performance points through a graphic procedure, which compares a structure's ability to resist lateral forces with a seismic demand, represented by a reduced elastic spectrum. The method is set out in ATC-40 (1996) [52]; however, FEMA 440 (2005) [53] introduced modifications which were considered in this research.

The values of the displacements obtained from the different cases studied, to obtain the performance points *IO*, *LS* and *CP*, are shown in Tab. 11.

Table 11 Performance points (*IO*, *LS* and *CP*) of the capacity curves

	Bare Frame	Block A	Block B	Block C	Block D
	X/*Y* direction				
IO / m	0.110/ 0.100	0.013/ 0.020	0.012/ 0.020	0.012/ 0.027	0.015/ 0.029
LS / m	0.142/ 0.128	0.017/ 0.025	0.016/ 0.026	0.016/ 0.035	0.019/ 0.037
CP / m	0.246/ 0.222	0.030/ 0.044	0.028/ 0.045	0.027/ 0.060	0.032/ 0.064

5.3 Thermal Analysis

A thermal analysis was carried out, using the results obtained in the laboratory for each block and the thermal transmittances shown in Tab. 9. The thermal analysis carried out used the unified software LIDER-CALENER (HULC) [54], which facilitates the verification of CTE DB-HE 2019 [55], issuing a report for the Energy Certification of buildings. This program is used to obtain urban planning licenses in Spain and its use is mandatory, according to Royal Decree 732/2019 [56]. For this purpose, a model of a single-family home was used, with the dimensions corresponding to Fig. 11 and using the standard materials and thicknesses used by the software for each envelope. The change produced in each model occurred in the enclosures, using the thermal characteristics obtained from the laboratory testing in this research (Tab. 9).

The details of the enclosures and the flat roof used in the model are shown in Fig. 16, with the corresponding thicknesses. The total width of the enclosure was 29 cm. The construction details of the building's roof, floors and walls (in contact with the ground) and the window and door carpentry were the same in all the cases analysed. The exterior carpentry used in the doors and windows was made of aluminium with a thermal break of 4-12 mm and low-emissivity double glazing 4/6/4.

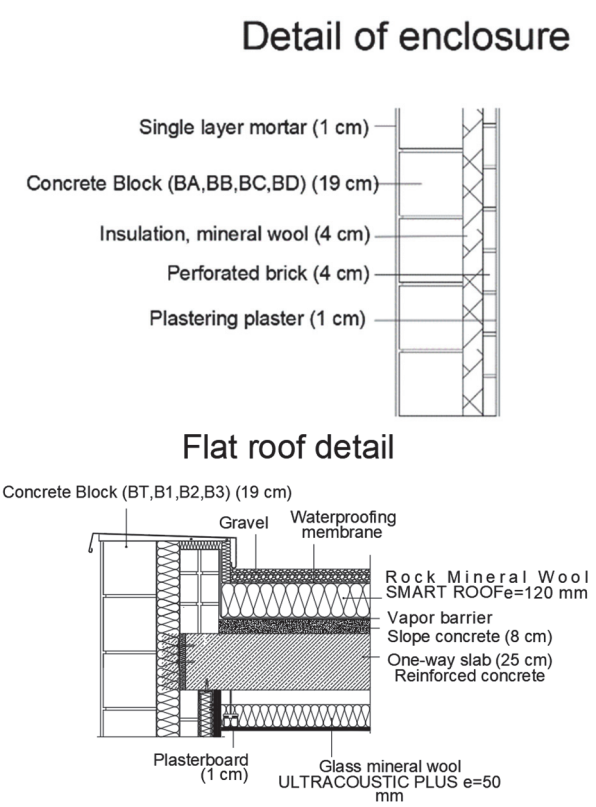

Figure 16 Detail of the enclosures and flat roof used in the model

The results obtained, in energy terms, using the blocks tested in this research, are those shown in Tab. 12. The values in parentheses show the existing relationship with respect to traditional blocks (A).

Table 12 Energy results

	Units	Block A	Block B	Block C	Block D
		Heating			
Demand, *D*	kWh/m^2 year	9.29	9.02 (−3%)	8.77 (−6%)	8.68 (−7%)
Final energy C_{Ef}	kWh/m^2 year	14.59	14.13 (−3%)	13.83 (−5%)	13.64 (−7%)
Emissions, E_{CO2}	kgCO_2/m^2 year	0.27	0.27	0.26 (−4%)	0.25 (−8%)

The results show a decrease in heating energy demand and CO_2 emissions in the construction modelled with a higher amount of recycled rubber and glass aggregates in the composition of the blocks.

6 CONCLUSIONS

The laboratory results of the blocks show the following:

1. Blocks with rubber and glass aggregates increase their compressive strength by 10%, with a percentage of 0.625% aggregates (block B) of rubber and glass, compared to the traditional block. However, higher percentages of these aggregates reduce their strength by 4% and 11%, at contents of 1.25% and 2.50%, respectively. This would be justified by the optimal amounts of additive added to the mixture, due to the lower compressive strength of rubber compared to concrete and the adhesion of glass and rubber in the mixture, as has been verified in other research.
2. Blocks with glass and rubber aggregates increase their flexural-tensile strength compared to traditional blocks, by 7% and 13% with glass and rubber aggregates. However,

these increases do not occur progressively; at a percentage of 2.50%, their strength decreases by 6% compared to 1.25% of aggregates.

3. Blocks with glass and rubber aggregates decrease their permeability, compared to traditional blocks, with a higher percentage of glass and rubber aggregates. These decreases are 7%, 11% and 17% as the percentages of glass and rubber additives are higher, with respect to the percentages analysed in this research.

4. Blocks with glass and rubber aggregates are more insulating because the percentages of glass and rubber are higher. Thermal conductivities are reduced by 19%, 29% and 36% because the percentages of glass and rubber additives are higher.

5. The densities of the blocks are reduced as the increase in glass and rubber increases. These reductions are 2%, 5% and 7%, respectively, with respect to the traditional block (BT).

On the other hand, considering the structural analyses carried out on the models with the characteristics defined in this research, the following can be concluded:

1. There are no major differences in the structural sections of the cases with walls. Even so, the structures that use blocks A (traditional block) and B (0.625% glass and rubber) are the most resistant of all the structures analysed. However, the resistance does not increase progressively with the addition of glass and rubber; percentages higher than 0.625% decrease it. Percentages exceeding 0.625% of rubber and glass additives reduce the structural strength of structural frames. On the other hand, the effectiveness of the blocks is evident when compared with the bare structures; the ultimate resistance increases considerably in both directions.

2. Analysing the ductility and elastic rigidity of the different structures in both directions, the most ductile solutions correspond to block D and the least ductile to the case that uses block B. On the other hand, the cases with the highest elastic rigidities correspond to the structures that use blocks A and B. The addition of a greater quantity of rubber and glass fibres considerably increases the ductility of the structures. The increase in ductility can be due to the characteristics of the new material or the infill wall as a whole. Increased ductility in frame structures with infill walls improves the seismic resistance of buildings, primarily due to: the absorption of energy by the structures during seismic movements, the fact that the structure deforms without breaking (brittle structures pose a risk to human life, a criterion contrary to that stated in seismic-resistant building codes worldwide), and damping. This quality does not mean that the structures have greater strength, as has been demonstrated.

3. The displacements of the structures with walls are considerably reduced due to the greater rigidity that the block walls inflict on the bare structures.

4. The performance points between the cases with block walls are similar, with the lowest displacements corresponding to the structures with blocks A and B. On the other hand, if these points are compared with the performance points of the buildings without walls, they are considerably reduced, to almost 90% in the *X* direction and 20% in the *Y* direction, with respect to the most favourable cases.

5. Considering the energy demand of the structures and the changing blocks, the structures with blocks containing recycled rubber and glass aggregates reduce this by 3%, 6% and 7%, with respect to a traditional block. In the same way, CO_2 emissions are also reduced by 4% and 8%, with respect to a traditional block.

For future studies related to this research, the optimal quantities of glass and rubber in the mixtures could be analyzed. Additionally, a study of the independent structural behavior of the walls in frame structures could be conducted.

Acknowledgements

This work is supported by the Chilean National Commission on Research and Development (ANID) [FONDECYT REGULAR grant number 1240156].

7 REFERENCES

[1] Oviedo-Cogollo, A. & Vega-Sánchez, J. (2021). Manejo de residuos de construcción y demolición y economía circular: Revisión narrativa. *Lámpsakos*, *26*, 41-51. https://doi.org/10.21501/21454086.4232

[2] Borsani, M. S. (2011). *Materiales ecológicos: Estrategias, alcance y aplicación de los materiales ecológicos como generadores de hábitats urbanos sostenibles*. Universitat Politècnica de Catalunya.

[3] Bustamante, W., Rozas, Y., Cepeda, R., Encinas, F., & Martínez, P. (2009). *Guía de diseño para la eficiencia energética en la vivienda social*. Ministerio de Vivienda y Urbanismo.

[4] D'Alençon, R., Justiniano, C., Márquez, F., & Valderrama, C. (2008). Parámetros y estándares de habitabilidad: Calidad en la vivienda, el entorno inmediato y el conjunto habitacional. *Camino al Bicentenario: Propuestas para Chile*, 271-304.

[5] García, A. N. D., Gil, R. E. R., & Rico, L. E. G. (2015). Impactos ambientales asociados con el proceso de producción del concreto. *Enfoque UTE*, *6*(4), 67-80. https://doi.org/10.29019/enfoqueute.v6n4.79

[6] Dávalos, A. (2013). Hormigón sustentable: Una nueva mirada a los materiales de construcción. *Beauchef Mag*, *5*, 19-22.

[7] Roussy, G. A. & Gattavara, H. M. (2018). *Pruebas de aditivos en hormigón*. Universidad Nacional de Córdoba.

[8] Ghedan, R. H. & Hamza, D. M. (2011). Effect of rubber treatment on compressive strength and thermal conductivity of modified rubberized concrete. *Journal of Engineering and Sustainable Development*, *15*(4), 21-29.

[9] Mushunje, K., Otieno, M., & Ballim, Y. (2018). A review of waste tyre rubber as an alternative concrete constituent material. *MATEC Web of Conferences*, *199*, 11003. https://doi.org/10.1051/matecconf/201819911003

[10] Jasim, A. T. & Abdulabbas, Z. H. (2020). Production of sustainable pervious concrete by using waste tires rubber as partial replacement of coarse aggregate. *AIP Conference Proceedings*, *2213*, 020221. https://doi.org/10.1063/5.0000255

[11] Instituto Nacional de Normalización. (2006). *NCh 181:2006, Bloques de hormigón para uso estructural-Requisitos generales*.

[12] Instituto Nacional de Normalización. (2016). *NCh 170:2016, Hormigón-Requisitos generales*.

[13] Instituto Nacional de Normalización. (1995). *NCh 2182:1995, Hormigón y mortero-Aditivos-Clasificación y requisitos*.

[14] Arteaga, C. J. C. (2013). *Estudio de la influencia del vidrio molido en hormigones grado H15, H20 y H30*. Valdivia, Chile.
[15] Soberón Monja, B. B. (2019). *Estudio sobre el efecto del vidrio reciclado molido en las propiedades ingenieriles de los principales materiales de construcción*. Universidad Católica Santo Toribio de Mogrovejo.
[16] Rodríguez, M. & Caturelli, M. E. R. (2016). Evaluación del desempeño de un hormigón con incorporación de vidrio reciclado finamente molido en reemplazo de cemento mediante ensayos de laboratorio. *Revista de la Facultad de Ciencias Exactas, Físicas y Naturales*, *3*(2), 53-60.
[17] Garcés Vargas, J. F. & Flores De la Rosa, V. (2016). Estudio del polvo de vidrio obtenido de la molienda de botellas recicladas como sustituto parcial del cemento en el hormigón. *Revista de Ciencia y Tecnología*, *3*(3). https://doi.org/10.26423/rctu.v3i3.195
[18] Cobeña, J. M. M., García, K. B. A., & Párraga, W. E. R. (2022). Estudio comparativo entre bloques artesanales y bloques elaborados con vidrio reciclado acorde a la norma INEN. *Polo del Conocimiento*, *7*(10), 434-455.
[19] Peñafiel Carrillo, D. A. (2016). *Análisis de la resistencia a la compresión del hormigón al emplear vidrio reciclado molido en reemplazo parcial del agregado fino*. Universidad Técnica de Ambato.
[20] Muñoz, S. & Mendoza, S. (2022). Diseño de mortero para albañilería incorporando vidrio reciclado triturado. *Revista Ingeniería de Construcción*, *37*(3), 391-404. https://doi.org/10.7764/RIC.00042.21
[21] Arrieta-Ballén, Y. L. & Pérez-Oyola, J. C. (2017). *Estudio para caracterizar una mezcla de concreto con caucho reciclado en un 5% en peso comparado con una mezcla de concreto tradicional de 3500 PSI*. Universidad de Cartagena.
[22] Ambrosio León, A. Q. (2020). *Resistencia a la compresión del ladrillo de concreto sustituyendo parcialmente el confitillo por caucho reciclado en un 5% y 10%*. Universidad San Pedro.
[23] Escalante Herrera, V. & Quintero Tinco, M. (2019). *Influencia de las fibras de caucho reciclado en la resistencia al corte no drenado de los suelos arcillosos expansivos*. Universidad César Vallejo.
[24] Gómez, F. & Donatilda, J. (2019). *Uso de caucho reciclado y tereftalato de polietileno (PET) para la elaboración de ladrillos ecológicos a nivel artesanal en el distrito de Chorrillos*. Universidad César Vallejo.
[25] Odian, G. (2004). *Principles of polymerization (4th ed.)*. John Wiley & Sons. https://doi.org/10.1002/047147875X
[26] Torres Ospina, H. A. (2014). *Valoración de propiedades mecánicas y de durabilidad de concreto adicionado con residuos de llantas de caucho*. Escuela Colombiana de Ingeniería Julio Garavito.
[27] Farfán, M. & Leonardo, E. (2018). Caucho reciclado en la resistencia a la compresión y flexión de concreto modificado con aditivo plastificante. *Revista Ingeniería de Construcción*, *33*(3), 241-250. https://doi.org/10.4067/S0718-50732018000300241
[28] Albano, C., Camacho, N., Hernández, M., Bravo, A. J., & Guevara, H. (2008). Estudio de concreto elaborado con caucho reciclado de diferentes tamaños de partículas. *Revista de la Facultad de Ingeniería Universidad Central de Venezuela*, *23*(1), 67-75.
[29] Instituto Nacional de Normalización. (1995). *NCh 182:1995, Bloques de hormigón para uso estructural*.
[30] Instituto Nacional de Normalización. (2009). *NCh 1038:2009, Hormigón-Ensayo de tracción por flexión*.
[31] Instituto Nacional de Normalización. (2007). *NCh 853:2007, Acondicionamiento térmico-Envolvente térmica de edificios-Cálculo de resistencias y transmitancias térmicas*.
[32] Mander, J. B., Priestley, M. J. N., & Park, R. (1988). Theoretical stress-strain model for confined concrete. *Journal of Structural Engineering*, *114*(8), 1804-1826. https://doi.org/10.1061/(ASCE)0733-9445(1988)114:8(1804)
[33] Bosco, M., Ferrara, E., Ghersi, A., Marino, E. M., & Rossi, P. P. (2016). Improvement of the model proposed by Menegotto and Pinto for steel. *Engineering Structures*, *124*, 442-456. https://doi.org/10.1016/j.engstruct.2016.06.037
[34] Zienkiewicz, O. C. & Taylor, R. L. (2005). *The finite element method for solid and structural mechanics (6th ed.)*. Elsevier. https://doi.org/10.1016/C2009-0-26332-X
[35] Paulay, T. & Priestley, M. J. N. (1992). *Seismic design of reinforced concrete and masonry buildings*. John Wiley & Sons. https://doi.org/10.1002/9780470172841
[36] Scott, M. H. & Fenves, G. L. (2006). Plastic hinge integration methods for force-based beam-column elements. *Journal of Structural Engineering*, *132*(2), 244-252. https://doi.org/10.1061/(ASCE)0733-9445(2006)132:2(244)
[37] Scott, M. H., Fenves, G. L., McKenna, F., & Filippou, F. C. (2008). Software patterns for nonlinear beam-column models. *Journal of Structural Engineering*, *134*(4), 562-571. https://doi.org/10.1061/(ASCE)0733-9445(2008)134:4(562)
[38] Spacone, E. & Filippou, F. (1996). Flexibility-based frame models for nonlinear dynamic analysis. *Proceedings of the 11th World Conference on Earthquake Engineering*, 23-28.
[39] SeismoSoft. (2021). *SeismoStruct (Version 2021)*. Computer software.
[40] Aslani, H., Cabrera, C., & Rahnama, M. (2012). Analysis of the sources of uncertainty for portfolio-level earthquake loss estimation. *Earthquake Engineering & Structural Dynamics*, *41*(11), 1549-1568. https://doi.org/10.1002/eqe.2230
[41] Kent, D. C. & Park, R. (1971). Flexural members with confined concrete. *Journal of the Structural Division*, *97*(7), 1969-1990. https://doi.org/10.1061/JSDEAG.0002957
[42] Mergos, P. E. & Kappos, A. J. (2015). Estimating fixed-end rotations of reinforced concrete members at yielding and ultimate. *Structural Concrete*, *16*(4), 537-545. https://doi.org/10.1002/suco.201400067
[43] British Standards Institution. (2005). *Eurocode 8: Design of structures for earthquake resistance-Part 1: General rules, seismic actions and rules for buildings (EN 1998-1)*.
[44] Domínguez, D., López-Almansa, F., & Benavent-Climent, A. (2014). Comportamiento, para el terremoto de Lorca de 11-05-2011, de edificios de vigas planas proyectados sin tener en cuenta la acción sísmica. *Informes de la Construcción*, *66*(533), e012. https://doi.org/10.3989/ic.12.092
[45] Iu, C. K. & Bradford, M. A. (2012). Higher-order non-linear analysis of steel structures. Part II: Refined plastic hinge formulation. *Advanced Steel Construction*, *8*(2), 183-198. https://doi.org/10.18057/IJASC.2012.8.2.5
[46] Attalla, M. R., Deierlein, G. G., & McGuire, W. (1994). Spread of plasticity: Quasi-plastic-hinge approach. *Journal of Structural Engineering*, *120*(8), 2451-2473. https://doi.org/10.1061/(ASCE)0733-9445(1994)120:8(2451)
[47] Liew, J. R., Chen, H., Shanmugam, N. E., & Chen, W. F. (2000). Improved nonlinear plastic hinge analysis of space frame structures. *Engineering Structures*, *22*(10), 1324-1338. https://doi.org/10.1016/S0141-0296(99)00085-1
[48] Valentini, F. & Pegoretti, A. (2022). End-of-life options of tyres: A review. *Advanced Industrial and Engineering Polymer Research*, *5*(4), 203-213. https://doi.org/10.1016/j.aiepr.2022.08.006
[49] Steyn, Z. C., Babafemi, A. J., Fataar, H., & Combrinck, R. (2021). Concrete containing waste recycled glass, plastic and rubber as sand replacement. *Construction and Building Materials*, *269*, 121242. https://doi.org/10.1016/j.conbuildmat.2020.121242
[50] Ma, Q., Mao, Z., Lei, M., Zhang, J., Luo, Z., Li, S., Du, G., & Li, Y. (2023). Experimental investigation of concrete

prepared with waste rubber and waste glass. *Ceramics International*, *49*(11), 16951-16970. https://doi.org/10.1016/j.ceramint.2023.02.058

[51] Structural Engineers Association of California. (2000). *Performance-based seismic engineering of buildings*. SEAOC.

[52] Comartin, C. D. (1996). *Seismic evaluation and retrofit of concrete buildings (Vol. 40)*. Seismic Safety Commission, State of California. https://doi.org/10.1193/1.1586093

[53] Federal Emergency Management Agency. (2005). *Improvement of nonlinear static seismic analysis procedures (FEMA 440)*. FEMA.

[54] Ministerio de Fomento. (2017). *Herramienta Unificada LIDER-CALENER (HULC), versión 1.0.1564.1124*. Computer software. Gobierno de España.

[55] Ministerio de Industria, Energía y Turismo. *Código técnico de la edificación: Documento básico de ahorro de energía (DB-HE)*. Gobierno de España.

[56] Hedo, E. B. (2020). Real Decreto 732/2019, de 20 de diciembre, por el que se modifica el Código Técnico de la Edificación. *Actualidad Jurídica Ambiental*, *97*, 84-86.

[57] Helmy, S. H., Tahwia, A. M., Mahdy, M. G., Abd Elrahman, M., Abed, M. A., & Youssf, O. (2023). The use of recycled tire rubber, crushed glass, and crushed clay brick in lightweight concrete production: A review. *Sustainability*, *15*(13), 10060. https://doi.org/10.3390/su151310060

[58] Xi, Y., Li, Y., Xie, Z., & Lee, J. S. (2004). Utilization of solid wastes (waste glass and rubber particles) as aggregates in concrete. *International Workshop on Sustainable Development and Concrete Technology*, 45-52.

[59] Jubeh, A. I., Al Saffar, D. M., & Tayeh, B. A. (2019). Effect of recycled glass powder on properties of cementitious materials containing styrene-butadiene rubber. *Arabian Journal of Geosciences*, *12*(2), 39. https://doi.org/10.1007/s12517-018-4212-0

[60] Martínez-Molina, W., Torres-Acosta, A. A., Alonso-Guzmán, E. M., Chávez-García, H. L., Hernández-Barrios, H., Lara-Gómez, C. et al. (2015). Concreto reciclado: Una revisión. *Revista Alconpat*, *5*(3), 235-248. https://doi.org/10.21041/ra.v5i3.91

[61] Tran, C. N., Illankoon, I. C. S., & Tam, V. W. (2025). Decoding Concrete's Environmental Impact: A Path Toward Sustainable Construction. *Buildings*, *15*(3), 442. https://doi.org/10.3390/buildings15030442

[62] Rangrazian, M., Madandoust, R., Mahjoub, R., & Raftari, M. (2023). Reduction of CO_2 environmental pollution from concrete by adding local mineral pozzolan as partial cement replacement: A case study on engineering properties. *Nanotechnology for Environmental Engineering*, *8*(1), 253-268. https://doi.org/10.1007/s41204-022-00288-4

[63] Liu, K., Tan, Q., Yu, J., & Wang, M. (2023). A global perspective on e-waste recycling. *Circular Economy*, *2*(1), 100028. https://doi.org/10.1016/j.cec.2023.100028

[64] Valdés Vidal, G., Reyes-Ortiz, Ó. J., & González Penuela, G. (2011). Aplicación de los residuos de hormigón en materiales de construcción. *Ingeniería y Desarrollo*, *29*(1), 17-33.

[65] Soto Prado, M. A. & Villegas Ponce, K. D. (2019) *Influencia de las proporciones de los agregados en el hormigón y la dosificación con cemento sobre el peso unitario y la resistencia a la compresión en un concreto convencional*. Universidad Nacional de Trujillo.

[66] Celik, O. C. (2016). Effect of AAC infill walls on structural system dynamics of a concrete building. *Journal of Earthquake Engineering*, *20*(5), 738-748. https://doi.org/10.1080/13632469.2015.1104757

[67] Lagaros, N. D., Naziris, I. A., & Papadrakakis, M. (2009). The influence of masonry infill walls in the framework of the performance-based design. *Journal of Earthquake Engineering*, *14*(1), 57-79. https://doi.org/10.1080/13632460902988976

[68] Crisafulli, F. J., Carr, A. J., & Park, R. (2000). Analytical modelling of infilled frame structures: A general review. *Bulletin of the New Zealand Society for Earthquake Engineering*, *33*(1), 30-47. https://doi.org/10.5459/bnzsee.33.1.30-47

[69] Crisafulli, F. J. & Carr, A. J. (2007). Proposed macro-model for the analysis of infilled frame structures. *Bulletin of the New Zealand Society for Earthquake Engineering*, *40*(2), 69-77. https://doi.org/10.5459/bnzsee.40.2.69-77

[70] Crisafulli, F. J. (1997). *Seismic behaviour of reinforced concrete structures with masonry infills*. University of Canterbury.

[71] Calvi, G. M., Priestley, M. J. N., & Kowalsky, M. J. (2007). Displacement-based seismic design of structures. *Proceedings of the New Zealand Conference on Earthquake Engineering*. https://doi.org/10.1193/1.2932170

[72] Huang, L., Zhou, Z., Zhang, Z., & Huang, X. (2021). Seismic performance and fragility analyses of self-centering prestressed concrete frames with infill walls. *Journal of Earthquake Engineering*, *25*(3), 535-565. https://doi.org/10.1080/13632469.2018.1526142

[73] Chopra, A. K. (1995). *Dynamics of structures: Theory and applications to earthquake engineering*. Prentice Hall.

[74] Instituto Nacional de Normalización. (2022). *NCh 1498:2022, Hormigón y mortero-Agua de amasado-Requisitos*.

[75] Instituto Nacional de Normalización. (2013). *NCh 163:2013, Áridos para morteros y hormigones-Requisitos generales*.

[76] Instituto Nacional de Normalización. (2016). *NCh 148:2016, Cemento-Terminología, clasificación y especificaciones generales*.

[77] Golewski, G. L. (2023). Assessing water absorption of concrete composites containing fly ash up to 30% for structures completely immersed in water. *Case Studies in Construction Materials*, *19*, e02337. https://doi.org/10.1016/j.cscm.2023.e02337

[78] Asokan, P., Osmani, M., & Price, A. D. (2009). Assessing the recycling potential of glass fibre reinforced plastic waste in concrete and cement composites. *Journal of Cleaner Production*, *17*(9), 821-829. https://doi.org/10.1016/j.jclepro.2008.12.004

[79] Li, X., Ling, T. C., & Mo, K. H. (2020). Functions and impacts of plastic/rubber wastes as eco-friendly aggregate in concrete-A review. *Construction and building materials*, *240*, 117869. https://doi.org/10.1016/j.conbuildmat.2019.117869

[80] Rahat Dahmardeh, S., Sargazi Moghaddam, M. S., & Mirabi Moghaddam, M. H. (2021). Effects of waste glass and rubber on self-compacting concrete: Rheological, mechanical, and durability properties. *European Journal of Environmental and Civil Engineering*, *25*(2), 302-321. https://doi.org/10.1080/19648189.2018.1528891

[81] Ma, Q., Mao, Z., Zhang, J., Du, G., & Li, Y. (2023). Behavior evaluation of concrete made with waste rubber and waste glass after elevated temperatures. *Journal of Building Engineering*, *78*, 107639. https://doi.org/10.1016/j.jobe.2023.107639

[82] Parghi, A. & Alam, M. S. (2016). Physical and mechanical properties of cementitious composites containing recycled glass powder and styrene-butadiene rubber. *Construction and Building Materials*, *104*, 34-43. https://doi.org/10.1016/j.conbuildmat.2015.12.006

[83] Ho, L. S. & Huynh, T. P. (2022). Recycled waste medical glass as a fine aggregate replacement in low environmental impact concrete: Effects on long-term strength and durability performance. *Journal of Cleaner Production*, *368*, 133144. https://doi.org/10.1016/j.jclepro.2022.133144

[84] Saghafi Lasemi, R., Ziaei, M., Alizadeh Elizei, M. H., & Esmaeil Abadi, R. (2024). Mechanical and thermal behaviour of concrete with waste rubber and glass powder as

fine aggregate and cement substitutes. *Magazine of Concrete Research*, *76*(9), 438-454. https://doi.org/10.1680/jmacr.23.00115

[85] Hameed, A. M. & Hamada, R. F. (2020). Using glass and rubber waste as sustainable materials to prepare foamed concrete with improved properties. *IOP Conference Series: Materials Science and Engineering*, *881*, 012188). https://doi.org/10.1088/1757-899X/881/1/012188

[86] Su, H., Yang, J., Ling, T. C., Ghataora, G. S., & Dirar, S. (2015). Properties of concrete prepared with waste tyre rubber particles of uniform and varying sizes. *Journal of Cleaner Production*, *91*, 288-296. https://doi.org/10.1016/j.jclepro.2014.12.022

[87] Güneyisi, E., Gesoğlu, M., & Özturan, T. (2004). Properties of rubberized concretes containing silica fume. *Cement and Concrete Research*, *34*(12), 2309-2317. https://doi.org/10.1016/j.cemconres.2004.04.005

[88] Gupta, T., Chaudhary, S., & Sharma, R. K. (2016). Mechanical and durability properties of waste rubber fiber concrete with and without silica fume. *Journal of Cleaner Production*, *112*, 702-711. https://doi.org/10.1016/j.jclepro.2015.07.081

[89] López-Almansa, F., Domínguez, D., & Benavent-Climent, A. (2013). Vulnerability analysis of reinforced concrete buildings with wide beams located in moderate seismicity regions. *Engineering Structures*, *46*, 687-702. https://doi.org/10.1016/j.engstruct.2012.08.033

[90] Domínguez, D., López-Almansa, F., & Benavent-Climent, A. (2014). Comportamiento, para el terremoto de Lorca de 11-05-2011, de edificios de vigas planas proyectados sin tener en cuenta la acción sísmica. *Informes de la Construcción*, *66*(533), e009. https://doi.org/10.3989/ic.12.062

[91] Pallares, F. J., Domínguez, D., & Pallares, L. (2020). Resilient structures in the seismic retrofitting of reinforced concrete frames: A case study. *Structural Engineering and Mechanics*, *76*(1), 57-65.

[92] Muñoz, P., Domínguez, D., Morales, M. P., Muñoz, L., & Sánchez-Vázquez, R. (2021). The effect of infill walls made of eco-materials on mechanical response, energy performance, and CO_2 footprint of low-rise buildings. *Energy and Buildings*, *243*, 110996. https://doi.org/10.1016/j.enbuild.2021.110996

[93] Domínguez-Santos, D. & Bravo, J. A. M. (2022). Structural and mechanical performance of adobe with the addition of high-density polyethylene fibres for the construction of low-rise buildings. *Engineering Failure Analysis*, *139*, 106461. https://doi.org/10.1016/j.engfailanal.2022.106461

Contact information:

D. DOMÍNGUEZ-SANTOS
(Corresponding author)
Department of Engineering and Building Management, University of Talca, Curicó, 3340000 Chile
E-mail: ddominguez@utalca.cl

Francisca E. SEPÚLVEDA LAGOS
Department of Engineering and Building Management, University of Talca, Curicó, 3340000 Chile
E-mail: fsepulveda17@alumnos.utalca.cl